Mapping the Actions of Microtubule Interfering Agents on Mitotic Signalling Pathways by Kinetworks™ Analysis

Hong Zhang*, Xiaoqing Shi**, Harry Paddon** and Steven Pelech**

*Kinexus Bioinformatics Corporation, Vancouver, B.C. Canada;
**Dept. Medicine, University of British Columbia, Vancouver, B.C. Canada

Abstract

Kinexus has developed its Kinetworks™ proteomics services with highly validated antibodies to provide precise and reliable data about the expression levels and phosphorylation states of hundreds of signalling proteins in tissue and cell lysates. Microtubule-interfering agents (MIA) such as nocodazole, taxol and vinblastine have been at the forefront of cancer chemotherapy due to the fundamental role that microtubules play in chromosomal segregation during mitosis. Kinetworks™ analysis was employed to investigate protein phosphorylation in MIA-treated human tumour cell lines that differed in their p53 status and susceptibility to apoptosis. In particular, MIA induced phosphorylation and activation of the MAP kinase JNK required functional p53, and interference of JNK function markedly enhanced tumour cell killing by these drugs. Nocodazole treatment triggered many other phosphorylation events, including the phosphorylation of STAT3 at Ser-727, which correlated with its activation and supports a previously unrecognized role for this transcription factor in mitosis. One of the many cross-reactive phosphoproteins that were also stimulated in phosphorylation by nocodazole in HeLa cells was purified and identified by mass spectrometry as the abundant nuclear protein B23 or nucleophosmin. MIA treatments were shown to increase phosphorylation of B23 at Ser-4. Conversion of Ser-4 to a glutamic acid residue to mimic constitutive phosphorylation of B23 prevented chromosome condensation *in vitro* and *in vivo*. The phosphorylation of STAT3 and B23 were shown to be mediated by

utility of the Kinetworks™ approach for pathway mapping.

Introduction

With the completion of the sequencing of the human genome, the most challenging and fruitful biomedical research endeavor of this decade will be the mapping of cell signalling systems and establishing their linkages to normal and disease related processes. At least 518 human protein kinases appear to be responsible for the phosphorylation of about 10,000 different proteins. Our knowledge of the architecture of protein kinase signalling networks is extremely rudimentary, but the application of systems biology approaches promises to reveal the true complexity of these networks. To this end, Kinexus has tested more than 1500 commercial antibodies for the accurate and quantitative detection of protein kinases and other signalling proteins in our Kinetworks™ immunoblotting services. With this methodology, we have previously reported novel interactions amongst protein kinases, including the binding of phosphorylated and activated p38 MAP kinase to the ERK1 and ERK2 MAP kinases to prevent their phosphorylation and activation by MEK1 and MEK2 [Zhang et al. (2001) J. Biol. Chem. 276:6905]. We also observed the direct binding of p38 MAP kinase to casein kinase 2, and demonstrated that this mediated the phosphorylation of the tumour suppressor protein p53 at Ser-392 to promote its activation [Sayed et al. (2000) J. Biol. Chem. 275:16569; Sayed et al. (2001) Oncogene 20:6994]. In the present study, we sought to further investigate the phosphorylation pathways that mediate the actions of inhibitors of microtubule dynamics such as nocodazole to block mitosis and induce apoptosis via p53 activation.

Materials & Methods

Total cell lysates were prepared from HCT-116 colon, HeLa cervical, MCF7 breast and A549 lung carcinoma cells following treatments with 200 ng/ml nocodazole, 1 µM vinblastine, or 1 µM colchicine for up to 72 h. Cells were washed with ice-cold PBS, scrapped in lysis buffer (20 mM Tris, 20 mM β-glycerophosphate, 150 mM NaCl, 3 mM EDTA, 3 mM EGTA, 1 mM Na_3VO_4, 0.5% Nonidet P-40, and 1 mM dithiothreitol) supplemented with 1 mM PMSF, 2 µg/ml leupeptin, 4 µg/ml aprotinin and 1 µg/ml pepstatin A, sonicated for 15 sec. Cell debris was removed by centrifugation at 100,000 rpm for 30 min at 4°C. Protein concentration was determined by the Bradford assay. For each Kinetwork™ analysis, 300-600 µg of total protein were resolved on a 13% single-lane SDS-polyacrylamide gel, transferred to nitrocellulose membrane. Using a 20-lane multiblotter, the membrane was incubated with different mixtures of up to 3 antibodies per lane that react with a distinct subset of 25-50 different pan-specific or phospho-site-specific signalling proteins of distinct molecular masses. After further incubation with a mixture of relevant HRP conjugated secondary antibodies, the blots were developed using ECL and signals were quantified using Quantity One software (Bio-Rad, Hercules, CA). Detailed information and protocols of the Kinetworks™ analysis have been published [Pelech et al. (2003) Methods in Molecular Medicine Series: Cancer Cell Signalling Kinetworks™ protein kinase multiblot analysis. (D. Terrian, ed.) vol. 218, 99-111 Humana Press] and can also be found at the Kinexus Bioinformatics Corp. website (www.kinexus.ca). All other standard protocols presented in this study have been published [Zhang et al. (2002) J. Biol. Chem. 277:43648].

Results

Treatment of HCT-116 cells with 200 ng/ml nocodazole induces a much stronger apoptotic response in p53+/+ cells than in p53-/- cells as revealed by genomic DNA fragmentation assay or flow cytometry (data not shown). To examine the signalling pathways downstream of p53 that might account for the difference in apoptosis induction, we applied various Kinetworks™ analyses. Figure 1 shows the results of a Kinetworks KPSS 1.0 phosphoprotein screen. Of greatest interest was the p53-dependent differential phosphorylation of the MAP kinases p40 JNK and p47 JNK at their activation sites. In the untreated p53-/- cells as compared to p53+/+ cells, there were marked reductions of the specific phosphorylations of p40 JNK (50-98%) and p47JNK (99%). While nocodazole treatment evoked clear stimulations of the specific phosphorylations of p40 JNK (2- to 4-fold), and p47 JNK (1.3-to 3-fold) in p53+/+ cells, no increases in JNK specific phosphorylation occurred following exposure of the p53-/- cells to nocodazole. These p53 loss of function-associated reductions in basal phosphorylation of JNK along with the abrogation of nocodazole-induced phosphorylation at these activating sites, revealed that JNK acts downstream of p53 in a signalling cascade in the HCT-116 p53+/+ cells. Figure 2 shows that the p53-dependent activation of JNK also occurs in other tumour cell types and in response to other MIA.

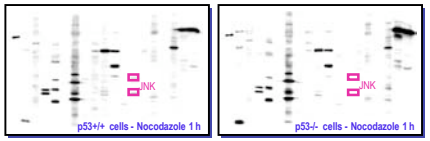

FIG. 1. Kinetworks™ KPSS 1.0 phosphoprotein analysis of HCT-116 cells.

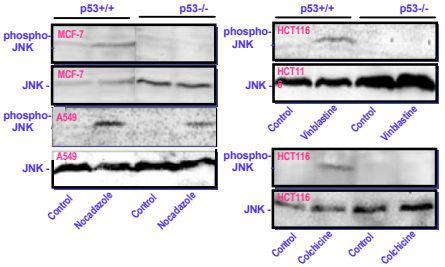

FIG. 2. p53-dependent nocodazole activation of JNK in MCF-7 breast and A549 lung cells. p53-dependent vinblastine and colchicine activation of JNK in HCT-116 cells. Note that the levels of JNK protein are higher in the p53/- or p53 inhibited cells, but MIA induce little or no phosphorylation of JNK at its activation site.

To address whether the differential JNK activation in response to nocodazole may account for the different sensitivity of p53+/+ and p53-/- cells to nocodazole induced cytotoxicity, we transfected p53+/+ cells with dominant negative mutants of four different p40 JNK isoforms, JNK1α(APF), JNK1β(APF), JNK2α(APF) and JNK2β (APF), individually, followed by a 1 h nocodazole treatment. No significant difference in p40 JNK activation was observed between empty vector-transfected control cells and each JNK(APF)-transfected cells upon nocodazole treatment (Fig. 3). Correlated with this, no apparent effect was seen on apoptosis induction after a 72 h nocodazole treatment in the cells transfected with each individual JNK(APF) mutant, as assessed by flow cytometry. However, when co-transfected with dominant negative mutants of all four different p40 JNK isoforms, p53+/+ cells exhibited about a 38% decrease in the phosphorylation of endogenous p40 JNK 1 h after nocodazole treatment as compared with vector-transfected control cells (Fig. 3). Surprisingly, a 1.7-fold increase in the number of apoptotic cells within 72 h after nocodazole treatment was detected in the p53+/+ cells co-transfected with all four dominant negative mutants.

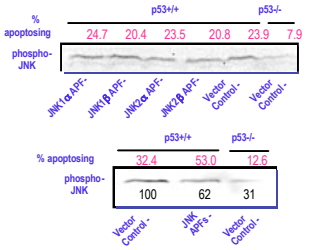

FIG. 3. JNK phosphorylation and apoptosis in HCT-116 cells transfected with dominant-negative forms of JNK.

SP600125 is a newly identified JNK inhibitor, and exhibits significant selectivity for JNKs. When a short-term treatment with both nocodazole and SP600125 was administrated, we observed inhibition of JNK and c-Jun phosphorylation in p53+/+ cells in response to 1 h SP600125 treatment as compared to nocodazole only treatment (data not shown). When treated with a combination of nocodazole and SP600125 for 72 h, a ~25% increase in apoptosis was observed in HCT116 p53+/+ cells, whereas no effect was found when SP600125 was used alone.

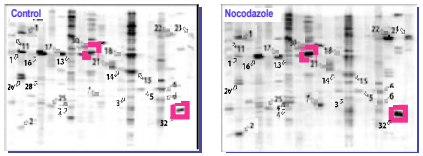

FIG. 4. HeLa cell phosphoproteins tracked in Kinetworks KPSS 1.2 Phospho-site Screen. Cells were treated with 100 ng/ml nocodazole for 20 h.

1. Adducin - S724
2. CDK1 - Y15
3. CREB - S133
4. ERK1/2 - T202/Y204
5. Gsk3α/β - S21/S9
6. Gsk3α/β - Y279/Y216
7. c-Jun - S73
8. MEK1 - S217/S221
9. MEK3/6 - S189/S207
10. MSK1 - S376
11. NR1 - S896
12. p38α - T180/Y182
13. p70 S6K - T389
14. PKBα - T308
15. PKBα - S473
16. PKCα - S657
17. PKCα - T638
18. PKCδ - T505
19. PKCε - S719
20. PKR - T451
21. Raf1 - S259
22. RB1 - S780
23. RB1 - S809/S811
24. Rsk1 - T360/S364
25. SAPK - T183/Y185
26. Smad1 - S463/S465
27. Src - Y416
28. Src - Y529
29. STAT1 - Y701
30. STAT3 - S727
31. STAT5 - S694
32. pp40

Exposing exponentially growing HeLa cells treated with 100 ng/ml nocodazole for 20 h resulted in mitotic arrest induced. As shown in Figure 4, Kinetworks™ KPSS 1.2 analysis revealed many expected changes (e.g. enhanced phosphorylation of CDK1 and RB), but surprisingly the screen also showed the increased phosphorylation of the transcription factor STAT3 at its Ser-727 activation site. Figure 5 demonstrates that several MIA could activate Ser-727 phosphorylation, and this could be inhibited by olomoucine, a drug that targets CDK1and CDK2. We have also demonstrated that seastar CDK1 can directly phosphorylate STAT3 at Ser-727, which indicates this may be a normal event during mitosis in HeLa cells.

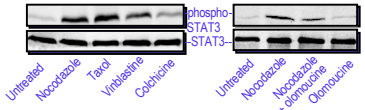

FIG. 5. MIA induced phosphorylation of STAT3 Ser-727 and its reduction by the CDK1 inhibitor olomoucine.

A ~40 kDa phosphoprotein (pp40) was consistently detected in HeLa cells by an antibody that was developed to recognize phospho-Mek1/2 (Ser-217/Ser-221), with at least 3 times higher intensity in nocodazole-treated cells as compared to serum-starved control cells (Fig. 4). To establish whether pp40 was a nocodazole-specific or a mitosis-associated protein, we monitored the level of pp40 in synchronized HeLa cells by releasing serum-starved cells from G0/G1 block with serum addition. A maximum level of pp40 was seen 24 h after serum addition, coinciding with the time when cyclin B1 was maximally expressed and CDK1 was maximally phosphorylated at its Thr-161 activation site, followed by a gradual decrease (Fig. 6). Similarly, pp40 was also detected in HEK 293, A549 and MCF-7 cells by the same antibody with higher abundance in mitotic cells than interphase cells (data not shown), indicating that the increase of pp40 was generally associated with mitosis. Following protein purification, pp40 was identified as the abundant nuclear phosphoprotein B23, also known as nucleophosmin. From alignment of the phospho-epitope for the Mek1/2 antibody with B23, Ser-4 was identified as the phosphorylation site, and this was confirmed by loss of the signal following alkaline phosphatase treatment and site-directed mutagenesis of this residue.

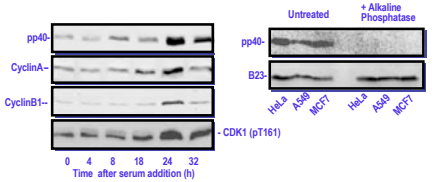

Mek1/2: ^{212}QLIDSMANSFVGTRSYMSPERLQ^{235}

B23WT: ^{1}MEDSMDMDMSPLRPQNYLFGCE^{22}

FIG. 6. Cell cycle dependent phosphorylation of pp40 in HeLa cells.

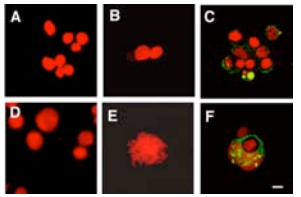

FIG. 7. Phosphorylation at Ser-4 of B23 regulations chromosome condensation. Scale bar, 100 µm

Mimicking Ser-4 phosphorylation by replacing the serine with a glutamic acid resulted in chromosome decondensation of HEK 293 nuclei both *in vivo* and *in vitro*, but exhibited no effect on subcellular localization of mutant proteins (Fig. 7). Expression of B23S4E (D), but not B23S4A (not shown) nor pcDNA empty vector (A), in HEK 293 cells for 72 h after transfection induced the expansion of nuclear areas. Incubating demembranated HEK 293 nuclei with GST-B23S4E protein (E), but not B23S4A (not shown) or GST (B) resulted in decondensation of nuclei after 30 min incubation at 37°C. Staining overexpressed B23S4E (F) and WT (C) proteins with anti-Flag antibody (green) in HEK 293 cells revealed no difference in localization of between mutant and wild-type proteins in either interphase or mitotic cells. Note: B23 is translocated into cytoplasm in mitotic cells with condensed chromosomes.

Acknowledgements --- We thank Dr. Bert Vogelstein (Johns Hopkins University) for providing HCT116 cell lines. We are also grateful to Drs. Kenji Fukasawa (University of Cincinnati), Xinmin Cao (National University of Singapore), Lynn Heasley (University of Colorado) and Jim Woodgett (Ontario Cancer Centre) for B23, STAT3 and JNK constructs, respectively.